

## Central Lancashire Online Knowledge (CLoK)

Title	Equation to Line the Borders of the Folding–Unfolding Transition Diagram of Lysozyme
Type	Article
URL	<a href="https://clock.uclan.ac.uk/15857/">https://clock.uclan.ac.uk/15857/</a>
DOI	<a href="https://doi.org/10.1021/acs.jpcc.6b01317">https://doi.org/10.1021/acs.jpcc.6b01317</a>
Date	2016
Citation	Mohammad, Mohammad Amin, Grimsey, Ian M. and Forbes, Robert Thomas (2016) Equation to Line the Borders of the Folding–Unfolding Transition Diagram of Lysozyme. <i>Journal of Physical Chemistry B</i> , 120 (28). pp. 6911-6916. ISSN 1520-6106
Creators	Mohammad, Mohammad Amin, Grimsey, Ian M. and Forbes, Robert Thomas

It is advisable to refer to the publisher's version if you intend to cite from the work.  
<https://doi.org/10.1021/acs.jpcc.6b01317>

For information about Research at UCLan please go to <http://www.uclan.ac.uk/research/>

All outputs in CLoK are protected by Intellectual Property Rights law, including Copyright law. Copyright, IPR and Moral Rights for the works on this site are retained by the individual authors and/or other copyright owners. Terms and conditions for use of this material are defined in the <http://clock.uclan.ac.uk/policies/>

1 **An Equation to Line the Borders of Folding-Unfolding Transition Diagram of Lysozyme**

2

3 Mohammad Amin Mohammad,<sup>\*,†,‡</sup> Ian M. Grimsey<sup>†</sup>, and Robert T. Forbes<sup>†,§</sup>

4 <sup>†</sup>Drug Delivery Group, School of Pharmacy, University of Bradford, Bradford BD7 1DP, UK.

5 <sup>‡</sup>Department of Pharmaceutics, Faculty of Pharmacy, University of Damascus, Damascus, Syria.

6 <sup>§</sup>School of Pharmacy and Biological Sciences, University of Central Lancashire, PR12HE, UK.

7

8 \* Corresponding author

9 Dr Mohammad Amin Mohammad

10 Associate Professor in Pharmaceutical Technology

11 First name: Mohammad Amin

12 Family name: Mohammad

13 Phone: + 44 (0)1225 386797

14 Email: [mam2014uk@gmail.com](mailto:mam2014uk@gmail.com)

15 Postal address: Dr. Mohammad Amin Mohammad, School of Pharmacy, University of Bradford,  
16 Bradford, West Yorkshire, BD7 1DP, UK.

17

18 Dr Ian M. Grimsey

19 Senior Lecturer in Pharmaceutical Technology

20 Phone: +44 (0)1274 234754

21 Fax: +44 (0)1274 234769

22 [i.m.grimsey@bradford.ac.uk](mailto:i.m.grimsey@bradford.ac.uk)

23 School of Pharmacy

24 University of Bradford

25 Bradford, West Yorkshire, BD7 1DP.

26

27 Prof Robert T. Forbes

28 Professor of Clinical Pharmaceutics

29 Phone: +44 (0)1772 893513

30 [rtforbes@uclan.ac.uk](mailto:rtforbes@uclan.ac.uk)

31 School of Pharmacy and Biomedical Sciences

32 University of Central Lancashire

33 Preston, Lancashire, PR1 2HE.

34

35

36

37

38

39

40 **ABSTRACT**

41

42 It is important for the formulators of biopharmaceuticals to predict the folding-unfolding transition  
43 of proteins. This enables them to process proteins at predetermined conditions without  
44 denaturation. Depending on apparent denaturation temperature ( $T_m$ ) of lysozyme, we have derived  
45 an equation describing its folding-unfolding transition diagram. According to water content and  
46 temperature, this diagram was divided into three different areas which are the area of the water-  
47 folded lysozyme phase, the area of the water-folded lysozyme phase and the bulk water phase, and  
48 the area of the denatured lysozyme phase. The amount of water content controlled the appearance  
49 and intensity of Raman band at  $\sim 1787\text{ cm}^{-1}$  when lysozyme powders were thermally denatured at  
50 temperatures higher than  $T_m$ .

51

52

53

54

55

56

57

58

59

60

61

62

## 63 INTRODUCTION

64

65 Protein structure and dynamics are determined by the intraprotein and protein-water non-  
66 covalent interactions.<sup>1,2</sup> Hydration degree of proteins, which is the weight ratio of water to protein,  
67 should be ~0.2 to initiate protein function, moreover, full protein function requires a hydration  
68 degree of ~1.<sup>3</sup> However, proteins are in their solid state during pharmaceutical processes and  
69 storage. Water contents of protein powders affect their stability and performance.<sup>4</sup> Water content  
70 alters the mechanisms of proteins' degradation reactions, and this alteration also depends on other  
71 conditions such as temperature and the formulation compositions.<sup>5</sup> In general, increasing water  
72 content decreases the stability of protein powders. Water acts as a plasticizer which enhances the  
73 molecular mobility of the proteins and so leads to an increase in their degradation rates. This  
74 shortens the shelf-life of solid protein powders and formulations.

75 Many studies have used lysozyme as a model protein to understand the effect of the water  
76 content on protein stability using differential scanning calorimetry (DSC). Previous works used  
77 sealed DSC pans to study the effect of water content on the glass transition temperature ( $T_g$ ) of  
78 lysozyme, they found that  $T_g$  of lysozyme decreased by increasing the water content to approach  
79 a plateau level.<sup>6,7</sup> Similarly, increasing water content within lysozyme powders decreased their  
80 apparent denaturation temperature ( $T_m$ ) in sealed DSC pans.<sup>8</sup> Therefore, both water content and  
81 temperature line the borders between the native (folded) and denatured (unfolded) states of  
82 lysozyme powders. These borders are important to predetermine the processing conditions (water  
83 content and temperature) which preserve the native structure of proteins during manufacturing  
84 processes (e.g., spray drying). Here, we derive an equation correlating water content of lysozyme  
85 powders with their  $T_m$ s, and then use this equation to line the borders of the folding-unfolding

86 transition diagram of lysozyme. Also, we use Raman spectroscopy to monitor water content effect  
87 on the molecular conformation of lysozyme upon the thermal unfolding transition of lysozyme  
88 powders.

89

## 90 **EXPERIMENTAL METHODS**

91

92 **Materials.** Lyophilized hen egg-white lysozyme powder (Biozyme Laboratories, UK) was  
93 purchased and considered to be unprocessed lysozyme powder.

94 **Sample Preparation.** The unprocessed lysozyme powder was used to prepare a series of  
95 lysozyme powders with different water contents either by raising or reducing their water content.  
96 The water residues were manipulated by exposing the powders to humidified air or to anhydrous  
97 nitrogen gas for different times at 30 °C. The prepared powders were immediately sealed and left  
98 to equilibrate at room temperature at least for a week after preparation. This time is enough to  
99 ensure uniformity of water distribution in lysozyme particles.<sup>9</sup> The prepared series of lysozyme  
100 powders were tested to correlate the water content with  $T_m$ . To monitor the water content effect  
101 on the molecular conformation of lysozyme upon the thermal unfolding transition, the lysozyme  
102 powders with different water contents were thermally denatured inside hermetically sealed pans  
103 by heating to temperatures higher than their unfolding transition peaks. These samples were  
104 considered to be the thermally denatured lysozyme powders.

105 **Thermogravimetric analysis (TGA).** The water content of each powder was determined  
106 using Thermo Gravimetric Analysis (TGA) (Perkin Elmer Ltd., UK). Samples (5-10 mg) were  
107 heated from 30 °C to 210 °C at a scan rate of 10 °C/min in an aluminum pan under nitrogen flow  
108 at 20 ml/min. Each sample was analyzed in triplicate. The decrease in the weight before

109 decomposition was considered as water content. TGA results were validated by re-analyzing the  
110 water content of some samples using Karl Fischer Titration (KFT) (701 KF Titrino with 703 Ti  
111 stand, Metrohm, Switzerland). Using TGA instead of KFT as only a few mg is enough for TGA.

112 **Differential scanning calorimetry (DSC).**  $T_m$  of each sample was measured using  
113 Differential Scanning Calorimetry (DSC) (Perkin-Elmer Ltd., UK). To study the effect of water  
114 residue on the thermal stability of lysozyme (the value of  $T_m$ ), the evaporation of water during  
115 heating was suppressed by using Large Volume Capsules, which are stainless steel sample  
116 containers equipped with an O-ring seal to provide a hermetic seal. Lysozyme powders (5-10mg)  
117 and solutions in water (20  $\mu$ l) were encapsulated in the hermetically sealed pans and scanned  
118 between 40 °C to 200 °C at 5 °C/min in triplicate. DSC was also used to prepare the thermally  
119 denatured lysozyme powders by heating them inside the hermetically sealed pans to temperatures  
120 higher than their unfolding transitions.

121 **FT-Raman spectroscopy.** FT-Raman spectra of the lysozyme powders at different water  
122 content and their thermally denatured lysozyme counterpart powders were recorded with a Bruker  
123 IFS66 optics system using a Bruker FRA 106 Raman module. The excitation source was an Nd:  
124 YAG laser operating at 1064 nm and a laser power of 50 mW was used. The FT-Raman module  
125 is equipped with a liquid nitrogen cooled germanium diode detector with an extended spectrum  
126 band width covering the wave number range 1850-1100  $\text{cm}^{-1}$ . Samples were placed in stainless  
127 steel sample cups and scanned 200 times with the resolution set at 8  $\text{cm}^{-1}$ . The observed band wave  
128 numbers were calibrated against the internal laser frequency and are correct to better than  $\pm 1 \text{ cm}^{-1}$ .  
129 <sup>1</sup>. The spectra were corrected for instrument response. The experiments were run at a controlled  
130 room temperature of 20  $\pm 1$  °C.

131

132 **Results and discussion**

133

134 We employed this protein because it folds in a highly cooperative manner and so exhibits  
135 an all-or-none thermal unfolding transition, and so it displayed one denaturation peak, in solid and  
136 solution states,<sup>10,11</sup> which makes the study easier. The driest prepared lysozyme powder contained  
137  $2.6 \pm 0.1$  %w/w water and its  $T_m$  was  $436.9 \pm 0.6$  K, while the wettest powder contained  $20.3 \pm 2.3$   
138 %w/w water and its  $T_m$  was  $355.5 \pm 3.1$  K. In Figure 1 is a DSC thermogram of each sample,  
139 showing an inverse correlation between water content and  $T_m$ s.

140

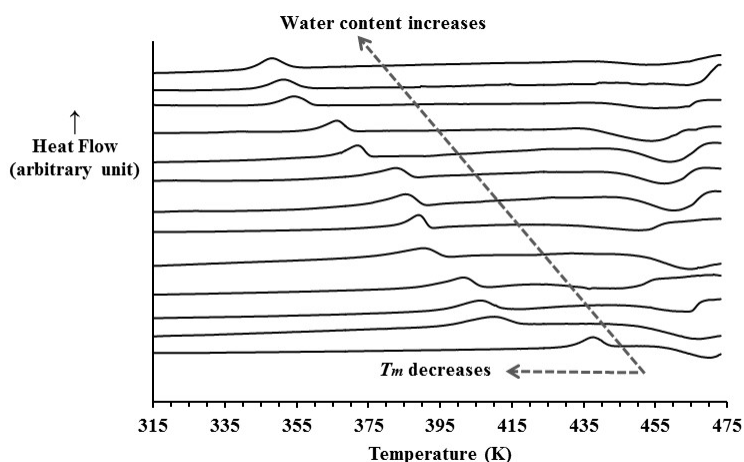


**Figure 1.** Differential scanning calorimetry thermograms of lysozyme powders (in sealed pans) at different water content.

141

142 Previous study demonstrated that DSC thermograms of lysozyme powders with different  
143 water content performed in pierced pans showed two endothermic peaks, the first broad peak,  
144 which extends from  $\sim 298$  to  $433$  K, indicates water evaporation and its area directly correlates to  
145 the water content, the second peak at  $\sim 473$  K refers to the protein denaturation ( $T_m$ ) and its position

146 is independent of water content because water evaporates through the pierced pans before the  
147 unfolding transition (denaturation) of lysozyme.<sup>10</sup>

148         However, unlike the experiments performed in the pierced pan, Figure 1 shows that the  
149 position of the endothermic unfolding peak ( $T_m$ ) varied for different water contents when DSC  
150 experiments were performed under sealed conditions. The DSC thermograms (Figure 1) did not  
151 show the water evaporation peak because the evaporation of water during heating was suppressed  
152 by the hermetical seal, i.e., the pressure generated from increasing the temperature of the air, which  
153 had been trapped during the capsulation of the hermetically sealed pans, prevented water loss.  
154 Figure 1 also show an exothermic peak after lysozyme unfolding in all samples analysed with the  
155 sealed pans. This peak was reproducible and showed little variation between samples, with a peak  
156 position ranging from 453 to 468 K. It was believed that this exothermic peak could be due to the  
157 aggregation of lysozyme molecules after unfolding, however re-scanning the sealed pans  
158 containing previously aggregated lysozyme powders also gave an exothermic peak at the same  
159 position but without the endothermic unfolding peak.

160         We hypothesized that water molecules associate with lysozyme powders to form a  
161 homogenous water-folded lysozyme phase. This phase unfolds at a kinetic thermal energy  
162 depending on water mole fraction ( $X_w$ ) and lysozyme mole fraction ( $X_p$ ) within the powders. When  
163  $X_w$  increases,  $T_m$  of the unfolding kinetic energy is reduced, and its reduction stops when the water  
164 molecules reach their saturation limit within the water-folded lysozyme phase. Above this limit,  
165 water molecules segregate from the water-folded lysozyme phase to form another phase of bulk  
166 water, and so they cannot reduce  $T_m$  further.

167          $X_w / X_p$  equals N, the ratio of water molecules to lysozyme molecules, and it is calculated  
168 according to Eq. (1):



169 
$$N = 14296 \times W\%/18 \times P\% \quad (1)$$

170 18 and 14296 are the molecular weights of water and lysozyme, respectively, and W% and P% are  
 171 the percentage of water weight and protein weight in the powders, respectively. The results were  
 172 tabulated in Table 1.

173

---

**Table 1.** The apparent denaturation temperature ( $T_m$ ), number of water molecules associating with one lysozyme molecule ( $N$ ), water mole fraction ( $X_w$ ) and lysozyme mole fraction ( $X_p$ ) of lysozyme powders at different water content.

Water content % w/w	$T_m$ (K)	$N$	$X_w$	$X_p$
2.5 (0.1)	436.9 (0.6)	20.4	0.9532	0.0468
4.6 (0.3)	412.0 (1.6)	38.1	0.9744	0.0256
5.2 (0.1)	406.2 (2.1)	43.4	0.9775	0.0225
6.4 (0.2)	401.9 (1.4)	54.3	0.9819	0.0181
7.7 (0.1)	390.3 (0.2)	66.6	0.9852	0.0148
8.5 (0.1)	388.8 (2.6)	73.8	0.9866	0.0134
9.2 (0.5)	385.5 (0.3)	80.5	0.9877	0.0123
9.9 (0.1)	383.5 (0.6)	87.7	0.9887	0.0113
12.0 (0.1)	371.8 (0.4)	108.7	0.9909	0.0091
14.4 (0.1)	365.7 (0.4)	133.1	0.9925	0.0075
15.6 (0.6)	364.0 (1.6)	146.6	0.9932	0.0068
20.3 (2.3)	355.5 (3.1)	201.8	0.9951	0.0049

Values within parenthesis are standard deviation, n = 3.

174

175  $T_m$  reflects the value of thermal kinetic energy needed to overcome the cohesion energy  
 176 stabilizing the folded state of proteins. This cohesion energy results from Van der Waals attraction,  
 177 electrostatic interaction, hydrogen bonding, and conformational entropy (hydrophobic effect).<sup>12</sup>  
 178 Electrostatic and hydrophobic interactions play the main roles in protein folding.<sup>1,13</sup> Water affects  
 179 these interactions and hence the magnitude of  $T_m$  needed to unfold proteins. Water molecules  
 180 surround the surface of protein molecules and penetrate into their cavities.<sup>14</sup> Surrounding water  
 181 molecules strengthen the hydrophobic effect by an increase in the entropy of water due to  
 182 association between hydrophobic residues.<sup>13</sup> However, according to Coulomb's law, the interior

183 waters weaken the electrostatic forces because they increase the dielectric constant in the interior  
 184 of protein molecules and also increase the distances between polarized and ionized groups of  
 185 proteins.<sup>15,16</sup> Our results demonstrated that the net effect of water weakens the forces responsible  
 186 for the folded state, and so the increased water content facilitates the protein unfolding at lower  
 187  $T_m$ . Dehydration of lysozyme powders stabilizes its native form because the free energy change of  
 188 the lysozyme denaturation increases by dehydration.<sup>17</sup>

189 Multiplying the gas constant ( $R$ ) by  $T_m$  gives the kinetic thermal energy needed to unfold  
 190 lysozyme. Interestingly, our data (Table 1) prove that  $RT_m$  and  $\ln N$  correlate linearly with a  
 191 correlation coefficient close to one ( $r = -0.997$ ), and their linear equation is:

$$192 \quad \ln N = \text{Slope } RT_m + \text{Intercept} \quad (2)$$

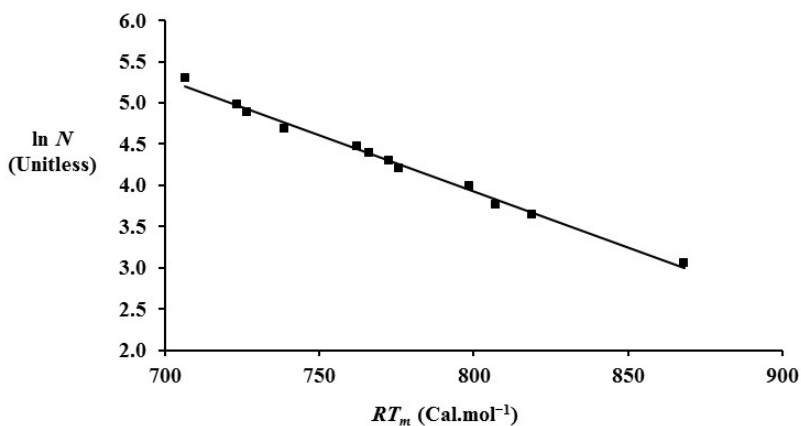
193 Figure 2 shows the straight line of Eq. (2) which was regressed in Eq. (3).

$$194 \quad \ln N = -\frac{RT_m}{72.3} + 15.0 \quad (3)$$

195 where 72.3 has units of  $\text{Cal.mole}^{-1}$  and 15.0 has units of  $\text{mole.mole}^{-1}$  (i.e., unitless).  $R = 1.9872041$   
 196  $\text{Cal.mole}^{-1}.\text{K}^{-1}$ , therefore Eq. (3) can be reduced to Eq. (4):

$$197 \quad T_m = -36.4 \ln N + 545.7 \quad (4)$$

198




---

**Figure 2.** The linear correlation between the denaturation thermal kinetic energy and logarithm of water molecules associating with one lysozyme molecule.

---

199 We measured  $T_m$ s of lysozyme solutions containing 80 %w/w and 70 %w/w of water.  $T_m$ s  
200 of the solutions were  $348.2\pm 0.7$  and  $348.0\pm 1.0$  K, respectively, and they were similar (T-test:  $P <$   
201  $0.05$ ). According to our hypothesis,  $T_m$  of the lysozyme solutions equals the apparent denaturation  
202 temperature of the saturated water-lysozyme phase ( $T_m^S$ ). Therefore, we extrapolated Eq. (4) to  $T_m^S$   
203 ( $348\text{K}$ ), which is the same as that of the solutions, to calculate the number of water molecules  
204 which saturate one molecule of lysozyme ( $N^S$ ) as follows:

$$205 \quad T_m^S = -36.4 \ln N^S + 545.7 \quad (5)$$

206 The calculated  $N^S$  was 228 water molecules according to Eq. (5). This water amount is equivalent  
207 to 22.3 %w/w and 0.3 g/g protein. We then prepared another lysozyme powder with a water content  
208 of  $23.2\pm 1.1$  %w/w, which is similar to the calculated  $N^S$ .  $T_m$  of the prepared water saturated  
209 powder was  $347.8\pm 1.4$  K, which is similar to  $T_m^S$  (T-test:  $P < 0.05$ ). Therefore, we used temperature  
210 and  $N$  to draw the folding-unfolding transition diagram of lysozyme. Figure 3 shows this diagram  
211 in which the denaturation line obeys Eq. (3) until reaching the water saturated solid state at  $N^S$ .  
212 After this value of water molecules,  $T_m$  did not significantly change. Our calculated value of  $N^S$ ,  
213 i.e. 228 water molecules, is similar to previously reported values of the hydration shell of  
214 lysozyme. Previous researchers used gigahertz to terahertz spectroscopy<sup>18,19</sup> Raman  
215 spectroscopy<sup>20</sup> neutron and X-ray scattering<sup>21</sup> NMR<sup>22</sup> to quantitate the hydration shell of  
216 lysozyme, and these methods estimated similar values of the hydration shell of lysozyme, and the  
217 values ranged between 170-270 water molecules. Hydration shell molecules have different  
218 properties from bulk water.<sup>23</sup> Our results demonstrate that the effect of water molecules on  $T_m$   
219 changed at  $N > N^S$ . Therefore, we speculate that water molecules begin to form the bulk water at  
220  $N > N^S$ . Therefore, the folding-unfolding transition diagram of lysozyme (As shown in Figure 3)  
221 was divided to three areas; (A) represents the area of the water-folded lysozyme phase, (B)

222 represents the area of the water-folded lysozyme phase and the bulk water phase, and (C)  
223 represents the area of the denatured lysozyme phase, and the line separating (C) from (A) and (B)  
224 is the denaturation line.  
225

---

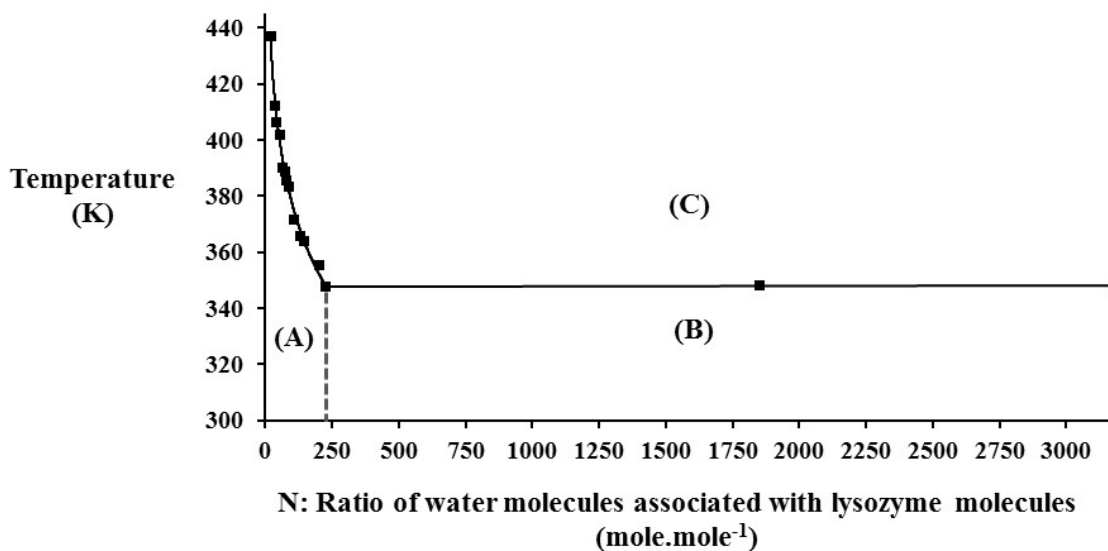


**Figure 3.** The folding-unfolding transition diagram of lysozyme. (A) represents the area of the water-folded lysozyme phase, (B) represents the area of the water-folded lysozyme phase and the bulk water phase, and (C) represents the area of the denatured lysozyme phase; the line separating (C) from (A) and (B) is the denaturation line.

---

226  
227 Although  $T_m$  of lysozyme solutions is usually  $\sim 348$  K, it changes due to additives (e.g., co-  
228 solvents, pH, ionic strength).<sup>10,24,25</sup> Also, additives changed  $T_m$  of lysozyme powders.<sup>8</sup> We could  
229 conclude that if the additives are miscible with water, they will participate in forming water-protein  
230 phases (in both solid and solution states). Therefore, they would change the constants of Eqs. (3)  
231 and (5). Whilst other proteins may have different constants.

232 Previous Raman study clarified the significant effects of hydration degree of native  
233 lysozyme powders on the back bone and the side chain conformations of lysozyme.<sup>9</sup> In other  
234 words, this previous study covered the molecular conformation of lysozyme under the denaturation

235 line of the folding-unfolding transition diagram of lysozyme. Here, the molecular conformation of  
236 lysozyme above the denaturation line were investigated. Raman spectra of the thermally denatured  
237 powders at different hydration degree and their original powders were collected at room  
238 temperature and presented in Figure 4. The peak intensities of the spectra were normalized using  
239 the band at  $1447\text{ cm}^{-1}$  (CH bending) as internal intensity standard. This is because its intensity and  
240 position are unaffected by changes induced in protein structure after applying different stresses.<sup>26</sup>  
241

---

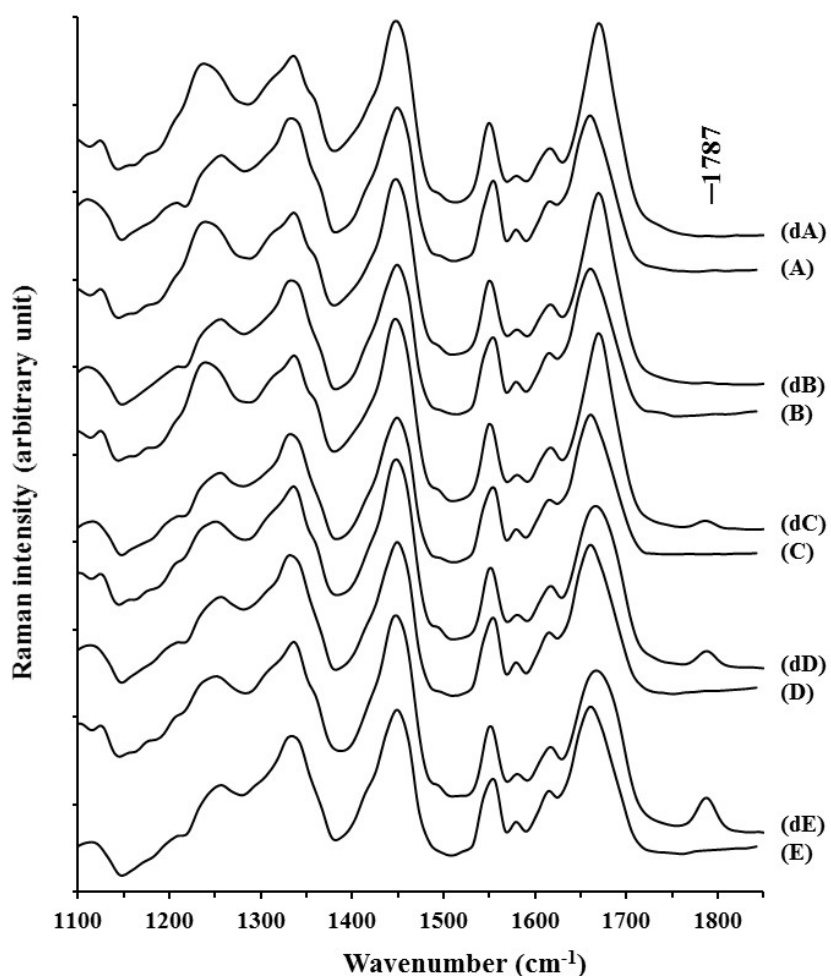


**Figure 4.** Representative Raman spectra of lysozyme powders in the  $1100\text{--}1850\text{ cm}^{-1}$  wavenumber region, (A), (B), (C), (D) and (E) represent lysozyme powders at different water content of 20.3, 12.0, 8.2, 5.2 and 2.5 %w/w, respectively, and (dA), (dB), (dC), (dD) and (dE) represent their thermally denatured counterpart powders (in sealed pans), respectively.

---

242           Within the investigated wavenumber region (1100–1850  $\text{cm}^{-1}$ ), we did not notice  
243 significant differences between the studied original lysozyme samples (Figure 4, spectra A, B, C,  
244 D and E). However, compared to the original lysozyme powders, the Raman spectra of the  
245 counterpart thermally denatured powders showed changes in the the peak positions of amide I and  
246 amide III bands. The peak of amide I was upshifted from  $\sim 1660$  to  $\sim 1671$   $\text{cm}^{-1}$  after thermal  
247 denaturation (Figure 4, spectra dA, dB, dC, dD and dE), and also spectra dD and dE show  
248 broadening in the amide I band in the case of the thermally denatured samples at low hydration  
249 degree (5.2 and 2.5 %w/w). The peak of amide III was downshifted from  $\sim 1256$  to  $\sim 1249$   $\text{cm}^{-1}$  at  
250 low hydration degree (spectra dD and dE), and it was further downshift to  $\sim 1240$   $\text{cm}^{-1}$  with an  
251 increase in the intensity at higher hydration degree (spectra dA, dB and dC). The Raman Bands of  
252 the amide I (C=O stretch) and amide III (N-H in-plane bend + C-N stretch) are indicators of the  
253 protein's secondary structures.<sup>9</sup> The mid-point of amide I is expected to be at  $1665 \pm 5$   $\text{cm}^{-1}$  for  $\alpha$ -  
254 helix and  $1670 \pm 3$   $\text{cm}^{-1}$  for  $\beta$ -sheet and disordered secondary structure, and the mid-point of amide  
255 III is expected to be at  $1267 \pm 8$   $\text{cm}^{-1}$  for  $\alpha$ -helix,  $1235 \pm 5$   $\text{cm}^{-1}$  for  $\beta$ -sheet and  $1245 \pm 4$   $\text{cm}^{-1}$  for  
256 disordered structure.<sup>27,28</sup> Therefore, the changes in Raman bands (presented in Figure 4) indicate  
257 that the content of the  $\beta$ -sheet and disordered secondary structure were increased and at the same  
258 time the  $\alpha$ -helix content was decreased after the thermal denaturation. Similar changes in the  
259 positions of amide I and amide III Raman bands of lysozyme powders were reported when  
260 lysozyme powders were denatured using mechanical stress<sup>10</sup> and  $\gamma$ -radiation<sup>29</sup>, and the researchers  
261 attributed these changes to a decrease in the  $\alpha$ -helix with an increase in the  $\beta$ -sheet and disordered  
262 structures. However, in the case of the thermally denatured powders, a new Raman band at  $\sim 1787$   
263  $\text{cm}^{-1}$  appeared, and its intensity decreased by raising the water content (Figure 4, spectra dC, dD  
264 and dE), and the peak disappeared at water content  $\geq 12$  %w/w (Figure 4, spectra dA and dB).

265 Therefore, the appearance of this peak at  $1787\text{ cm}^{-1}$  relates to the nature of lysozyme molecules'  
266 movement during the thermal unfolding transition and this movement depends heavily on the  
267 amount of hydration degree of the powders. The new band at  $1787\text{ cm}^{-1}$  could be assigned to the  
268 stretching of free hydrogen bonding carbonyl group. As the line of amide I at wavenumbers  $\geq 1685$   
269  $\text{cm}^{-1}$  is expected to be assigned to the disordered secondary structure without hydrogen bonding.<sup>27</sup>  
270 It can be concluded that the higher the water content in lysozyme powders during unfolding  
271 transition, the higher the freedom for lysozyme molecules to move and saturate the free carbonyl  
272 groups of the peptide bonds resulted from the unfolding transition. At water content  $\geq 12\text{ %w/w}$ ,  
273 the lysozyme molecules have enough freedom to move and saturated all the free carbonyl groups,  
274 and this explains the disappearance of the Raman band at  $1787\text{ cm}^{-1}$ . This finding agrees with  
275 previous results stating that at water content between 11 and 21  $\text{ %w/w}$ , lysozyme possess a  
276 glasslike dynamic transition from rigid to flexible state due to the mobility increase of the structural  
277 units.<sup>30</sup>

278 Therefore, the shape of amide I Raman band, the position and intensity of amide III Raman  
279 band, and the intensity of the Raman band at  $\sim 1787\text{ cm}^{-1}$  of the thermally denatured powders  
280 depend on the water content of their original native powders. This indicates that the molecular  
281 structure of the thermally denature lysozyme depends on its hydration degree.

282 This folding-unfolding transition diagram of lysozyme was obtained using sealed pans in  
283 order to ensure mass conservation of the water-lysozyme system. Therefore, it was determined at  
284 constant volume but variable pressure. Fortunately, in our case, we capsulated the sealed pans at  
285 atmospheric pressure ( $\sim 0.1\text{ MPa}$ ), and according to the general gas law, the increase in the pressure  
286 due to the temperature increase from 298 to 473 K inside the hermetically sealed pans would reach

287 ~0.2 MPa. This pressure values have a negligible role in the lysozyme denaturation. It was  
288 confirmed that lysozyme is denatured when pressure is at much higher values >500 MPa.<sup>31</sup>

289

## 290 **CONCLUSIONS**

291

292 These results allowed us to derive an equation correlating  $T_m$  of lysozyme with its  
293 hydration degree.  $T_m$  exponentially decreased when the hydration degree increased, and it did not  
294 significantly decrease further after hydration degree reaching a value similar to hydration shell of  
295 the lysozyme. We used the derived equation to draw the folding-unfolding transition diagram of  
296 lysozyme. This diagram will be useful to process lysozyme at predetermined conditions of  
297 temperature and water content without denaturation. The molecular conformation of the thermally  
298 denatured lysozyme was found to be dependent on the hydration degree of the original native  
299 powders. A new Raman band at  $1787\text{ cm}^{-1}$  appeared in the spectra of the thermally denatured  
300 lysozyme, and its intensity reversibly correlated with the water content and it disappeared at the  
301 water content  $\geq 12\text{ \%w/w}$ .

302

## 303 **AUTHOR INFORMATION**

304 Corresponding Author

305 \*E-mail: mam2014uk@gmail.com

306 Notes

307 The authors declare no competing financial interest.

308

309



310 **ACKNOWLEDGEMENTS**

311  
312 The authors thank Dr Ian S. Blagbrough (University of Bath) for helpful discussions. MAM  
313 gratefully acknowledges CARA (Stephen Wordsworth and Ryan Mundy) and University of  
314 Bradford for providing an academic fellowship.

315  
316 **REFERENCES**

- 317 (1) Ji, C.; Mei, Y. Some practical approaches to treating electrostatic polarization of proteins. *Acc.*  
318 *Chem. Res.* 2014, *47*, 2795–2803.
- 319 (2) Dhindsa, G. K.; Tyagi, M.; Chu, X. Q. Temperature-dependent dynamics of dry and hydrated  
320 beta-casein studied by quasielastic neutron scattering. *J. Phys. Chem. B* 2014, *118*, 10821–10829.
- 321 (3) Frauenfelder, H.; Chen, G.; Berendzen, J.; Fenimore, P. W.; Jansson, H.; McMahon, B. H.;  
322 Stroe, I. R.; Swenson, J.; Young, R. D. A unified model of protein dynamics. *Proc. Natl. Acad.*  
323 *Sci. U.S.A.* 2009, *106*, 5129–5134.
- 324 (4) Broadhead, J.; Rouan, S. K.; Hau, I.; Rhodes, C. T. The effect of process and formulation  
325 variables on the properties of spray-dried beta-galactosidase. *J. Pharmacol. Pharmacother.* 1994,  
326 *46*, 458–467.
- 327 (5) Wang, W. Lyophilization and development of solid protein pharmaceuticals. *Int. J. Pharm.*  
328 *2000*, *203*, 1–60.
- 329 (6) Miyazaki, Y.; Matsuo, T.; Suga, H. Low-temperature heat capacity and glassy behavior of  
330 lysozyme crystal. *J. Phys. Chem. B* 2000, *104*, 8044–8052.
- 331 (7) Panagopoulou, A.; Kyritsis, A.; Aravantinou, A. M.; Nanopoulos, D.; Serra, R. S. I.; Ribelles,  
332 J. L. G.; Shinyashiki, N.; Pissis, P. Glass transition and dynamics in lysozyme-water mixtures over  
333 wide ranges of composition. *Food Biophys.* 2011, *6*, 199–209.
- 334 (8) Bell, L. N.; Hageman, M. J.; Muraoka, L. M. Thermally induced denaturation of lyophilized  
335 bovine somatotropin and lysozyme as impacted by moisture and excipients. *J. Pharm. Sci.* 1995,  
336 *84*, 707–712.
- 337 (9) Kocherbitov, V.; Latynis, J.; Misiunas, A.; Barauskas, J.; Niaura, G. Hydration of lysozyme  
338 studied by Raman spectroscopy. *J. Phys. Chem. B* 2013, *117*, 4981–4992.
- 339 (10) Mohammad, M. A.; Grimsey, I. M.; Forbes, R. T. Mapping the solid-state properties of  
340 crystalline lysozyme during pharmaceutical unit-operations. *J. Pharm. Biomed. Anal.* 2015, *114*,  
341 176–183.
- 342 (11) Maroufi, B.; Ranjbar, B.; Khajeh, K.; Naderi-Manesh, H.; Yaghoubi, H. Structural studies of  
343 hen egg-white lysozyme dimer: comparison with monomer. *Biochim. Biophys. Acta* 2008, *1784*,  
344 1043–1049.
- 345 (12) Yano, Y. F. Kinetics of protein unfolding at interfaces. *J. Phys. Condens. Matter* 2012, *24*,  
346 503101–503117.
- 347 (13) Wu, Z.; Cui, Q.; Yethiraj, A. Driving force for the association of hydrophobic peptides: the  
348 importance of electrostatic interactions in coarse-grained water models. *J. Phys. Chem. Lett.* 2011,  
349 *2*, 1794–1798.

350 (14) Tilton, R. F. Jr.; Kuntz, I. D. Jr.; Petsko, G. A. Cavities in proteins: Structure of a  
351 metmyoglobin xenon complex solved to 1.9 Å. *Biochemistry* 1984, *23*, 2849–2857.

352 (15) Dwyer, J. J.; Gittis, A. G.; Karp, D. A.; Lattman, E. E.; Spencer, D. S.; Stites, W. E.; García-  
353 Moreno E, B. High apparent dielectric constants in the interior of a protein reflect water  
354 penetration. *Biophys. J.* 2000, *79*, 1610–1620.

355 (16) Pitera, J. W.; Faltus, M.; Van Gunsteren, W. F. Dielectric properties of proteins from  
356 simulation: the effects of solvent, ligands, pH, and temperature. *Biophys. J.* 2001, *80*, 2546–2555.

357 (17) Kocherbitov, V.; Arnebrant, T. Hydration of thermally denatured lysozyme studied by  
358 sorption calorimetry and differential scanning calorimetry. *J. Phys. Chem. B* 2006, *110*, 10144–  
359 10150.

360 (18) Vinh, N. Q.; Allen, S. J.; Plaxco, K. W. Dielectric spectroscopy of proteins as a quantitative  
361 experimental test of computational models of their low-frequency harmonic motions. *J. Am. Chem.*  
362 *Soc.* 2011, *133*, 8942–8947.

363 (19) Knab, J.; Chen, J. Y.; Markelz, A. Hydration dependence of conformational dielectric  
364 relaxation of lysozyme. *Biophys. J.* 2006, *90*, 2576–2581.

365 (20) Bellavia, G.; Paccou, L.; Achir, S.; Guinet, Y.; Siepmann, J.; Hédoux, A. Analysis of Bulk  
366 and Hydration Water During Thermal Lysozyme Denaturation Using Raman Scattering. *Food*  
367 *Biophys.* 2013, *8*, 170–176.

368 (21) Svergun, D. I.; Richard, S.; Koch, M. H. J.; Sayers, Z.; Kuprin, S.; Zaccai, G. Protein  
369 hydration in solution: experimental observation by x-ray and neutron scattering. *Proc. Natl. Acad.*  
370 *Sci. U.S.A.* 1998, *95*, 2267–2272.

371 (22) Kuntz, I. D. Hydration of macromolecules. III. Hydration of polypeptides. *J. Am. Chem. Soc.*  
372 1971, *93*, 514–516.

373 (23) Choudhuri, J. R.; Chandra, A. An ab initio molecular dynamics study of the hydrogen bonded  
374 structure, dynamics and vibrational spectral diffusion of water in the ion hydration shell of a  
375 superoxide ion. *Chem. Phys.* 2014, *445*, 105–112.

376 (24) Blumlein, A.; McManus, J. J. Reversible and non-reversible thermal denaturation of lysozyme  
377 with varying pH at low ionic strength. *Biochim. Biophys. Acta. Proteins and Proteomics* 2013,  
378 *1834*, 2064–2070.

379 (25) Chen, P.; Seabrook, S. A.; Epa, V. C.; Kurabayashi, K.; Barnard, A.S.; Winkler, D. A.; Kirby,  
380 J. K.; Ke, P. C. Contrasting effects of nanoparticle binding on protein denaturation. *J. Phys. Chem.*  
381 *C* 2014, *118*, 22069–22078.

382 (26) Yu, T. J.; Lippert, J. L.; Peticolas, W. L. Laser Raman studies of conformational variations of  
383 poly-L-lysine. *Biopolymers* 1973, *12*, 2161–2176.

384 (27) Li-Chan, E. C. Y. The applications of Raman spectroscopy in food science.  
385 *Trends. Food. Sci. Tech.* 1996, *7*, 361–370.

386 (28) Yu, N. T.; Liu, C. S. Laser Raman Spectra of Crystalline and Aqueous Glucagon. *J. AM.*  
387 *Chem. Soc.* 1972, *94*, 5127–5135.

388 (29) Torreggiani, A.; Tamba, M.; Manco, I.; Faraone-Mennella, M. R.; Ferreri, C.; Chatgililoglu,  
389 C. Radiation damage of lysozyme in a biomimetic model: some insights by Raman spectroscopy.  
390 *J. Mol. Struct.* 2005, *744*, 767–773.

391 (30) Kocherbitov, V.; Arnebrant, T.; Söderman, O. Lysozyme–water interactions studied by  
392 sorption calorimetry. *J. Phys. Chem. B* 2004, *108*, 19036–19042.

393 (31) Hédoux, A.; Guinet, Y.; Paccou, L. Analysis of the mechanism of lysozyme pressure  
394 denaturation from Raman spectroscopy investigations, and comparison with thermal denaturation.  
395 *J. Phys. Chem. B* 2011, *115*, 6740–6748.

$$T_m = -36.4 \ln N + 545.7 \text{ when } N \leq N^S$$

$$T_m \cong T_m^S \text{ when } N \geq N^S$$

$T_m$ : Apparent denaturation temperature of lysozyme.

N: Ratio of water molecules to lysozyme molecules.

S: Superscript refers to saturated water-lysozyme state.